IAEA
INTERNATIONAL ATOMIC ENERGY AGENCY
23nd IAEA Fusion Energy Conference
Daejeon, 11 - 16 October 2010

IAEA-CN-165/EX/1-1

HIGH CONFINEMENT HYBRID SCENARIO IN JET AND ITS SIGNIFICANCE FOR ITER

E. JOFFRIN 1) 4), C. CHALLIS 2), J. CITRIN 3), J. GARCIA 4), J. HOBIRK 5) , I. JENKINS 2), J. LONNROTH 2, D. C. MCDONALD 2) , P. MAGET 4) , P. MANTICA 6), M. BEURSKENS 2), M. BRIX 2), P. BURATTI 7), F. CRISANTI 7), L. FRASSINETTI 8), C. GIROUD 2), F. IMBEAUX 4), M. PIOVESAN), F. RIMINI 1), G. SERGIENKO 2), A.C.C. SIPS 1), T.TALA 9), I. VOITSEKOVITCH 2) AND JET EFDA CONTRIBUTORS(*)

JET-EFDA, Culham Science Centre, Abingdon OX14 3DB, UK.

1) JET-EFDA-CSU, Culham Science Centre, Abingdon, OX14 3DB, UK.
2) Euratom/CCFE Fusion Association, Culham Science Centre, Abingdon, OX14 3DB, UK.
3) FOM Institut for Plasma Physics Rijnhuizen, Association EURATOM-FOM, Nieuwegein.
4) CEA-IRFM, Association Euratom-CEA , Cadarache, F-13108, France.
5) Max-Planck-Institut fur Plasmaphysik, Euratom Association, 85748, Garching Germany.
6) Instituto di Fisica del Plasma CNR, EURATOM-ENEA-CNR Association, Milano, Italy.
7) Associazione EURATOM-ENEA sulla Fusione, C.R. Frascati, Frascati , Italy.
8) Association EURATOM-VR Fusion Plasma Physics EES, KTH, Stockholm, Sweden
9) Association EURATON-Tekes, VTT, PO Box 1000, FIN-02044 VTT Finland

***S**ee the Appendix of F. Romanelli et al., Fusion Energy 2008 (Proc. 22st Int. Conf. Geneva, 2008) IAEA, (2008)

High confinement hybrid scenario in JET and its significance for ITER

E. Joffrin 1) 4), C. Challis 2), J. Citrin 3), J. Garcia 4), J. Hobirk 5) , I. Jenkins 2), J. Lonnroth 2, D. C. McDonald 2) , P. Maget 4) , P. Mantica 6), M. Beurskens 2), M. Brix 2), P. Buratti 7), F. Crisanti 7), L. Frassinetti 8), C. Giroud 2), F. Imbeaux 4), M. Piovesan), F. Rimini 1), G, Sergienko 2), A.C.C. Sips 1), T.Tala 9), I. Voitsekovitch 2) and JET EFDA contributors(*)

1) JET-EFDA-CSU, Culham Science Centre, Abingdon, Oxfordshire, OX14 3DB, UK.
2) Euratom/CCFE Fusion Association, Culham Science Centre, Abingdon, OX14 3DB, UK.
3) FOM Institut for Plasma Physics Rijnhuizen, Association EURATOM-FOM, Nieuwegein.
4) CEA-IRFM, Association Euratom-CEA , Cadarache, F-13108, France.
5) Max-Planck-Institut fur Plasmaphysik, Euratom Association, 85748, Garching Germany.
6) Instituto di Fisica del Plasma CNR, EURATOM-ENEA-CNR Association, Milano, Italy.
7) Associazione EURATOM-ENEA sulla Fusione, C.R. Frascati, Frascati , Italy.
8) Association EURATOM-VR Fusion Plasma Physics EES, KTH, Stockholm, Sweden
9) Association EURATON-Tekes, VTT, PO Box 1000, FIN-02044 VTT Finland
Main author email: emmanuel.joffrin@jet.efda.org

Abstract: In the last campaigns, JET has extended the hybrid scenario with q profile close to unity in the plasma core to higher confinement (H_{98y2} up to 1.4-1.5) for both high and low triangularity. This has been achieved by creating a large region of weak magnetic in the plasma core. With these performances, 50% of the total current is generated non-inductively would produce in ITER a discharge of 1000s duration. The effect of this broad q profiles shape could reduce transport in the core in particular in the low shape scenario which also has the strongest rotation gradients. With broad q profile neoclassical tearing mode stability is shown to be improved. The pedestal does not seem to depend crucially on the modification of the magnetic shear, but shows a constant improvement with power and β. This improvement is more pronounced at low shape than low shape. High shapes can also be affected by high recycling flux that can impact on the pedestal confinement. Given the inapplicability of existing confinement scaling law at β_N higher than 2, the extrapolation of these scenarios to ITER is using instead a dimensionless approach. There is good prospect to produce in ITER long pulse operation with Q approaching 10 but there are large uncertainties in particular with respect to the role of rotation on transport.

1. Introduction

In the recent 2008-2009 campaigns, JET has achieved a comprehensive exploration of the plasma scenario, known as the “hybrid” scenario. In ITER, this scenario is a standard H-mode regime operated at slightly lower plasma current (typically 12 to 13.5MA instead of 15MA), with an H factor of 1 and aiming at reaching a fusion gain factor of typically Q=5 for duration exceeding 1000s because of the smaller demand on the available inductive flux.

Major progress have been achieved in JET in the preparation of the operation and physics basis of an ITER hybrid plasma: i) confinement factor with respect to the IPB98(y,2) scaling [1] have been observed up to levels of 1.4-1.5 for at least one resistive time, with β_N=3 at different normalised gyro-radii ρ* from 3.5×10^{-3} to 6×10^{-3}, ii) q profile access conditions to the scenario has been explored and non-inductive current requirements characterised, iii) a stable route with respect to neo-classical tearing modes (NTM) has been identified in terms of q profile, and iv) the origins of the reduced transport have been examined in details. On this basis, prediction to ITER can be strengthened in terms of confinement and operation, and recommendation can now be given in terms of q profile and required external non-inductive current.

This paper first presents an overview and description of the hybrid scenario at JET with high confinement and then presents the technique used to pre-form the target q profile (prior to the main heating) that led to these results. The current profile evolution is analysed and the consequences of the change of q the profile are then examined in details in terms of transport, stability and pedestal properties of the discharges. In the light of this analysis, the physics dependencies of the confinement scaling are then examined and a new extrapolation approach to ITER proposed and discussed.

2. JET hybrid scenario experiment overview

Initial JET experiments on the hybrid scenario did not lead in years 2003 and 2006 [2] to substantial increase of confinement with respect to the IPB98(y,2) scaling (H≲ 1). In the past two years, the experiments have been extended to larger variation of q profile keeping central

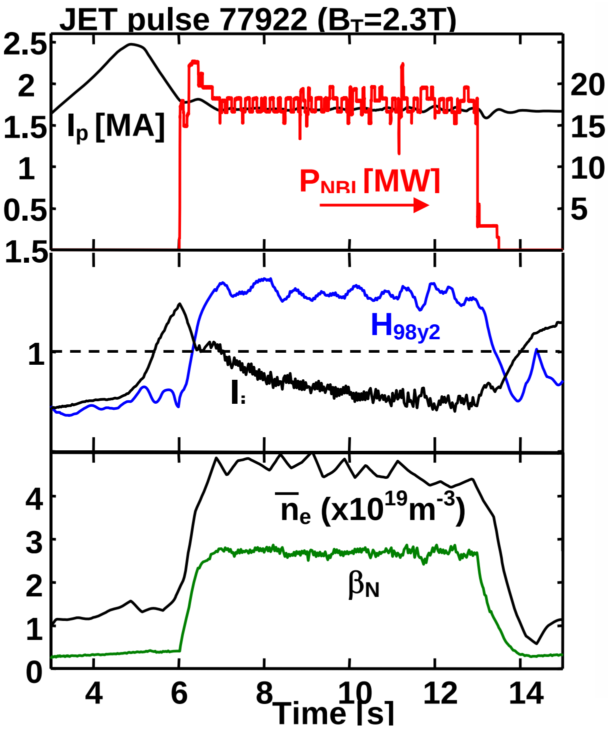

Fig 1: JET hybrid discharge (δ~0.4) at 75% of the Greenwald density with H_{98y2} reaching 1.3 for about one resistive time.

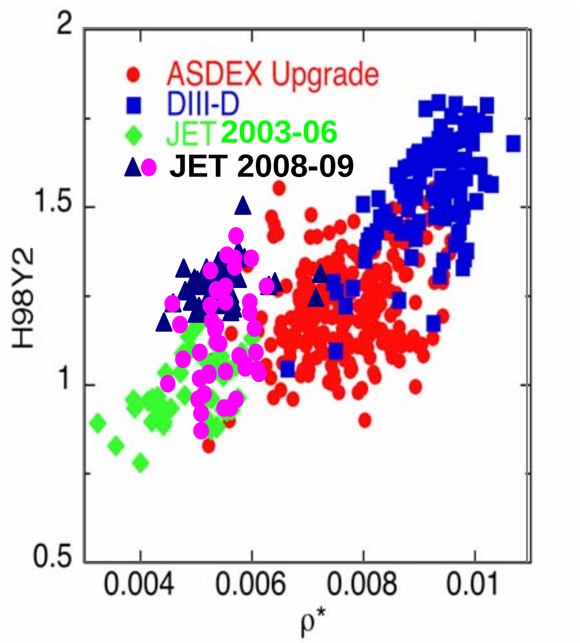

Fig 2: JET hybrid H_{98y2} factor versus ρ compared other devices (from ITPA database). Recent pulses achieved H factor up to 1.4-1.5 at both low shape (pink circles) and high shape (dark triangles).*

q_o close to 1. Confinement improvement up to H_{98y2}=1.4 have been achieved by broadening the current density profile (flat core q profile over a large part of the plasma radius) using current ramp down techniques prior to the main heating phase. This technique has been first applied successfully to low triangularity (δ=0.2) at low magnetic field strength (B_T=1.7T/Ip=1.4MA) and densities of the order of 50% of the Greenwald density. It has then be applied to high triangularity ITER-like shape (δ~0.4) and thus to higher density (75% of the Greenwald density) with H_{98y2}=1.3-1.4 and β_N~3 of the same order of 4xli. Finally these results have been extended to higher field (B_T=2.3T) and current (up to 2MA) and maintained for duration of typically one resistive time (τ_R) (fig 1). In all these scenarios, an Ip overshoot has the role of modifying the target q profile (at the time of the main heating) to a broad q profile prior to the main heating. Figure 1 illustrates this experiment and shows that the internal inductance peaks prior to the main heating and then decays towards a value of ~0.75. It can be observed that the H factor survives this last change. A constant value of β_N is maintained by feedback control using the neutral beam power.

Figure 2 shows a compilation of about hundred of these new JET discharges for both shapes in terms of the confinement factor versus ρ* determined as $(2MT)^{1/2}/aB$, where T is inferred from the total energy content W assuming Ti=Te. On this graph, it is apparent that the new data are reaching a level of confinement equivalent to what is obtained in ASDEX Upgrade, therefore breaking the apparent decreasing trend of the H factor with ρ* reported in [3]. However, it should be pointed out that this trend cannot be considered as a scaling since the other dimensionless parameters (ν*, β, and shape) are not kept constant in this data set. Recent dimensionless experiments made with the hybrid scenario between JET and DIII-D are clearly showing that there exists only a very weak dependence of H98y2 with ρ* [4].

3. Analysis of the current profile evolution in the JET hybrid scenario

Both CRONOS [5] and TRANSP [6] have been used to reconstruct the current evolution following the current overshoot. Both codes are reconstructing the current evolution

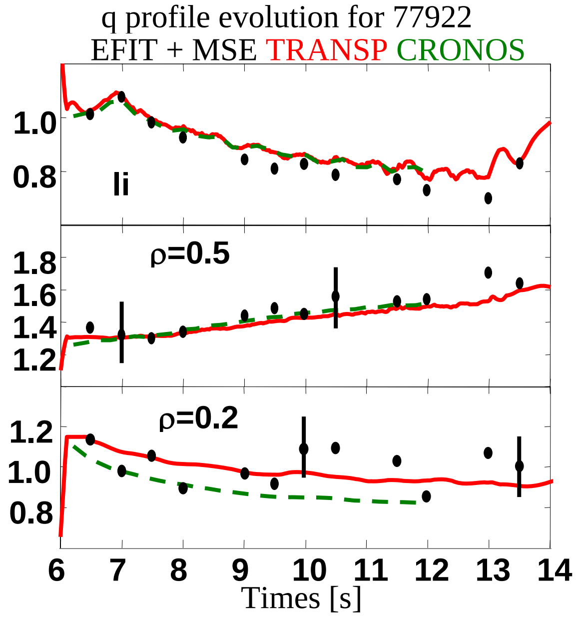

Figure 3a: li and q evolution at ρ=0.2 and 0.5 from EFIT + MSE (dots) and predicted by CRONOS (green dashed) and TRANSP (red) using the same initial conditions.

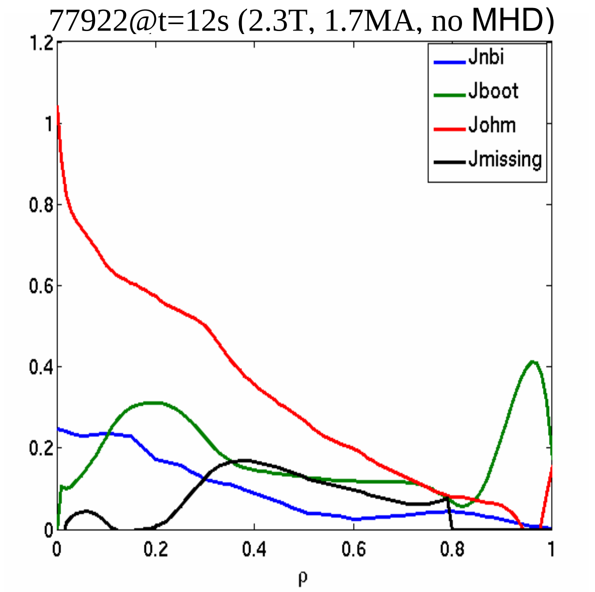

Fig 3b: current balance for hybrid scenario of figure 1 with q_{95}~4.3. The "missing" current refers to the external current drive required to achieve maintain the q profile constant at 12s.

consistently with the experimental inductance and the q profile evolution inferred from the equilibrium reconstruction using EFIT constrained by MSE data and the total pressure profile (fig 3a). This indicates that the q profile peaks with time during the main heating phase, after the Ip overshoot. In past experiments it had been reported [2] that JET hybrid did not have any anomalous central current diffusion in contrast to other machine such as DIII-D [7] and AUG [8]. For the more recent pulses, figure 3a also confirms that no anomaly is found with respect to the neoclassical theory. Inside r/a~3, the presence of a continuous n=1 activity with intermittent sawtooth is sometimes observed and the central q_o evolution is not always reproduced by the current diffusion codes. This suggests that this MHD activity is redistributing the magnetic flux inside its radius of location.

From these simulations the current balance analysis has been carried out (figure 3b) and shows typically 50% of non-inductive current (15% from beam driven current and 35% from bootstrap current). This level of non-inductive current would be compatible with a 1000s discharge duration in ITER. From this analysis, the non-inductive current necessary to maintain the stable q profile is quantified following the idea developed in [9]. The external current drive that should be provided is referred to as "missing current" in figure 6. That additional current would conserve the q

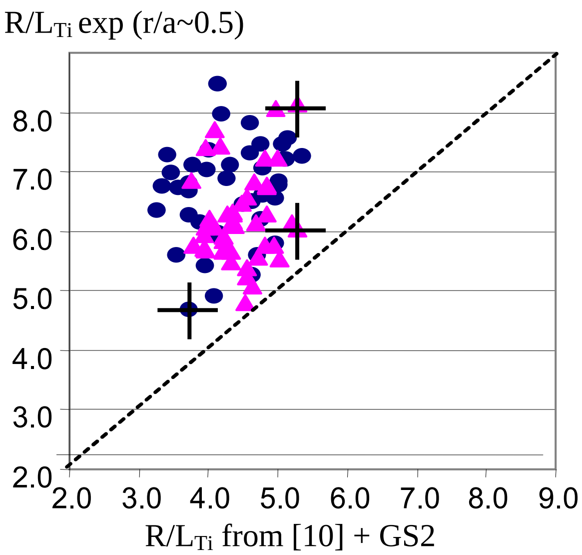

Fig 4: Comparison of the experimental ion gradient length versus the analytical formula from [10] for low shape (circles) and high shape (triangles) hybrid scenarios.

profile with stable MHD conditions at t=12s. This analysis indicates that off-axis (at r/a~0.5) current drive would be required to achieve a stable hybrid scenario.

4. Transport, stability and pedestal properties.

Given these results, the role of the q profile modifications reported above has been examined in terms of core transport, MHD stability, pedestal confinement and wall interaction.

Regarding core transport, the normalised gradients length R/L_{Ti} at r/a=0.5 have been characterised with respect to the critical gradient length predictions. The experimental gradient length are inferred from Thomson scattering for n_e, Te and Ti and rotation from charge exchange spectroscopy for all remapped onto the toroidal flux grid coordinate given by EFIT constrained with MSE data. These data are compared in Figure 4 with the prediction calculated using the analytical formula in [10] in the flat density limit ($R/Ln_e<2(1+Ti/Te)$ which is valid in this dataset. A renormalization coefficient for the absolute value has been applied by comparing the analytical formula with linear gyro-kinetic calculations from GS2 [11] for specific pulses. It appears that for both shapes the experimental gradient lengths are above the predicted values. Also, low shapes pulses have in average higher gradients length than high shape pulses. At the same time, these pulses are showing strong rotation gradients at r/a~0.5 (~810^4 rd/s/m for the high shape and up to 1.510^5 rd/s/m for the low shape), corresponding to Mach number of 0.45 and 0.55 respectively. All this is consistent with the hypothesis discussed in [12] that these plasmas are not stiff in the core and stiffness could be reduced by rotation, allowing for high T_i peaking at high rotation. The difference in T_i/T_e (T_i/T_e~1.8 for the low shape instead of ~1.3 for the high shape) also contributes to having larger R/L_{Ti} in low shape, by increasing the threshold, but this effect is quantitatively smaller and is already accounted for in the calculated threshold. Also, s/q (where s is the magnetic shear) is similar for both shapes (s/q~0.9 +/-0.2).

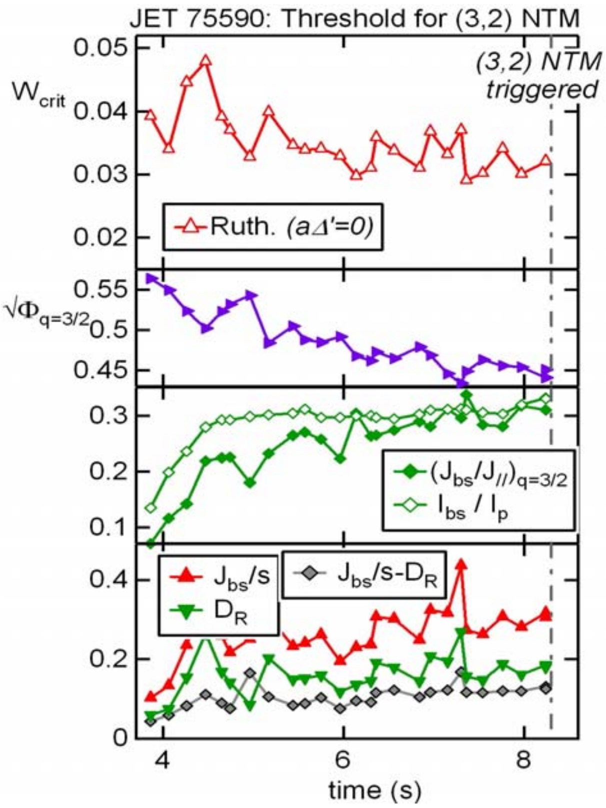

Fig 5: From top to bottom: evolution of the critical island width for the 3/2 mode (box 1), location of the rational surface (box 2), total and local bootstrap current at q=3/2 (box 3) and bootstrap destabilising and curvature term in the Rutherford equation (box 4).

These observations suggest that core transport may be reduced in particular for the low shape due to higher rotation in situation of core low magnetic shear, as discussed in [12]. This effect is not described in standard ion temperature gradient instability models (such as GLF23 [13]). Indeed, for the JET hybrid scenario this code appears to overestimate the experimental Ti when rotation (ExB shear stabilisation) is included. This would suggest that it does not capture correctly the effect of rotation on the critical ion gradient length or change of stiffness in the hybrid scenario.

The evolution of the q profiles in hybrid pulses after the Ip overshot has also revealed the behaviour of the tearing mode activity (or NTMs) as function of the q profile. Depending on the precise initial conditions (target q), the hybrid scenario can have successively 5/4, 4/3 and then 3/2 modes during the current diffusion phase, or have very mild MHD activity. Each of these modes are affecting the confinement (4/3 mode by ~5% and 3/2 mode by ~15%).

Plasmas with the highest confinement are often characterised by a continuous n=1 mode with infrequent or no sawteeth as observed in ASDEX Upgrade [14]. The stability of the unstable cases has been examined using the extended Rutherford equation framework including bootstrap (J_{bs}/s) and curvature (D_R) effects for determining the evolution of the island size Wcrit with time. From figure 5, it can be seen that during the current diffusion, the critical island width tends to decay and the rational surface 3/2 moves inwards towards the region of stronger pressure gradients. As a result the destabilising bootstrap current term (red trace last box) increases and overcomes the stabilising curvature terms gradually (green trace last box). The plasma becomes more vulnerable to the destabilisation of the 3/2 mode for any seed mechanism and eventually the 3/2 mode occurs at 8.2s in this case. From this stability analysis, it appears that maintaining a broad q profile is a necessary condition for the operation of stable hybrid scenario with respect to the neoclassical tearing modes.

As shown in figure 3a, the Ip overshoot produces a very strong modification of the current density in the outer half of the plasma resulting in significant changes of the edge shear where the edge transport barrier is established. Therefore the pedestal in hybrid scenario could be a key player in the overall confinement. A recent study exploiting the high resolution Thomson scattering capabilities show that the pedestal energy contribution is typically 40 to 30% of the total energy content for high shapes and 30 to 20% for low shape. These ratios are in line with what is found in no Ip overshoot (or baseline scenario) for the same total energy content. There are also indications that the pedestal energy in the hybrid scenario (i.e. with β_N~3) is stronger than for the baseline scenario (with β_N~2) for the same energy content as calculated by the H_{98y2} scaling [16]. In order to examine this point more in depth, a specific experiment has be designed where the input power (therefore β_N) was scanned at constant plasma current, toroidal field strength, density for both high and low shapes separately. The results shown in figure 6 suggest that i) the pedestal energy evolution with power does not seem to be affected by the Ip overshoot for both shapes within the pedestal measurement error bars ii) low shape αvδ high shapes $\beta_{e,ped}$ so not seem to increase with power with the same rate This last point is consistent with the trend seen in [17] suggesting that confinement scaling is more favourable with β at low shape. On-going modelling should show if this can be associated with the standard MHD ETB stability model, but from these first results, it appears that the Ip overshoot is not changing the pedestal confinement significantly.

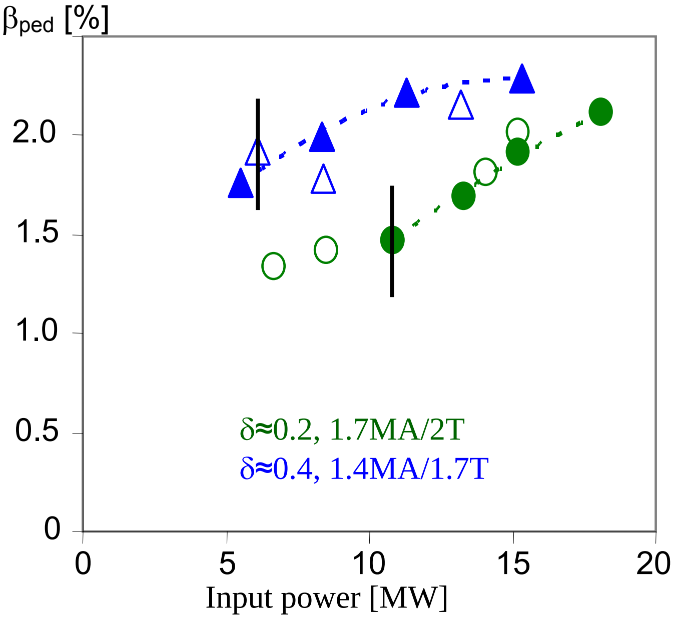

Figure 6: $\beta_{e,ped}$ at the pedestal top dependency on power for hybrid pulses with (solid symbols) and without Ip overshot (open symbols).

However, the comparison of past 2003-06 hybrid scenario data (see green symbols on figure 2) and recent data (see blue triangles on figure 2) at high shape has indicated that the pedestal energy is different for equivalent stored energy plasma current and field. This difference can be explained by the shape difference. The high δ shape used in past experiment could undergo stronger magnetic flux deformation with increasing Shafranov shift and interact with the machine top protection tiles. The comparative test of the two shapes in the same plasma conditions is showing that the recycling flux from Dα light was higher by a factor of 4 in the old magnetic configuration than in the recent configuration used in 2008-09. Thus the enhanced neutral flux from the wall to the plasma could affect the pedestal temperature and density (as observed by the Thomson scattering diagnostic) and reduce the pedestal confinement by charge exchange losses. EDGE2D [18] calculations are on-going to check this point, but this implies that shape optimisation has been an important factor in the recent results at high triangularity. The neutral interaction with plasma in a carbon wall machine is not unusual and could become very different in an all metallic wall device with tungsten and beryllium since the neutral recycling with these materials is known to be very different [19].

5. Extrapolation to ITER

It is uncertain whether the Ip overshot can be extrapolated in practice to a larger device or higher plasma current in JET and the access to the broad q profiles in ITER should be examined separately. However given the benefits brought to stability and transport properties, it important to examine how this improved scenario can be extrapolated in its main heating phase. Since plasmas in the hybrid domain show a global confinement enhancement compared with the H98y2 scaling, it is not clear that the dependencies of these scaling can be used to extrapolate hybrid plasma performance to the domain of future devices. In addition, this scaling has been derived using a large H-mode database [1] with β_{NTH} <2.2 and is therefore not applicable for discharge with β_{NTH} >2.2 as it is the case for the hybrid scenario.

H_{98y2} can be expressed in terms of dimensionless parameters ($\rho^* \sim (MT)^{1/2}/aB$, $\nu^* \sim qna/T^{-2}$, $\beta \sim nT/B^2$ and $q=q_{cyl}=5BR.\kappa\ /a^2Ip$) as: $B.\tau_E=\rho^{*-2.69}\ \nu^{*-0.01}\ \beta^{-0.90}\ q^{-3.0}$. This is derived assuming Ti=Te which is generally not the case in the type of beam heated plasmas shown above. In the JET hybrid scenarios at high triangularity Ti/Te is in average about 1.3, whereas it is expected to be 0.9 in ITER.

In JET the operational space of these improved confinement hybrid plasmas has been extended to different parameters such as q_{95} (from 3.5 to 5) and normalised gyro-radius ρ^* from 3 10^{-3} to 2.1 10^{-3} (i.e. $\rho^*/\rho^*_{ITER}\sim$ 2) at fixed shape (δ=0.4). When a least square regression is carried out on the database of JET hybrid pulses using the measured volume average ion temperature from charge exchange for the calculation of ρ^* and ν^*, the following dependences are found: $B.\tau_E \sim \rho^{*-2.02}\ \nu^{*-0.19}\ \beta^{-0.44}\ q^{-1.22}$

Although the database used is limited ($0.005<\rho^*<0.008$; $0.02<\nu^*<0.08$; $1.6\%<\beta<2.7\%$ and $2.3<q_{cyl}<3$), it is interesting to note that the dependencies found are close to the individual parameter scan for the ρ^* dependence (Bohm-like) found in recent between DIII-D and JET for similar discharges [20]. In addition, this expression is showing a ν^* dependence which is very different than H_{98y2} and closer to that obtained in dedicated collisionality and q_{cyl} scans (keeping the other terms constant) as reported in [21]. For example, specific experiments varying only ν^* in DIII-D and JET have found a dependence in $\nu^{*-0.35}$. This could impact significantly on the fusion prediction for the ITER hybrid scenario since $\nu^*_{JET}/\ \nu^*_{ITER}$ ~5 to 10.

Using the assumption Ti=Te for the same set of discharge leads to slightly different exponent: $B.\tau_E \sim \rho^{*-2.07}\ \nu^{*-0.10}\ \beta^{-0.41}\ q^{-1.26}$ but still not far from the exponents found using measured Ti within the error bars. Both would lead to a power degradation of $\sim P^{-0.5}$.

Given these considerations, an extrapolation to ITER has been performed using of one pulse (77933, Ip=2MA, B_T=2.3T, H_{98y2}=1.25) using a dimensionless approach. This is achieved in three successive steps:

i) Identity step scaling up to the ITER shape using: $n\sim a^{-2}$, $T\sim a^{-1/2}$. $Ip\sim a^{-1/4}$, $\omega_c\sim a^{-5/4}$.

ii) ρ^* step to ITER ρ^* using the ordering: $n\sim B^{-4/3}$, $T\sim B^{2/3}$, $Ip\sim B$, $\omega_c\sim B^{1/3}.a^{-5/6}$.

iii) νc step: $n\sim B^0$, $T\sim B^2$, $Ip\sim B$, $\omega_c\sim B$. Here $\nu_c\sim Rn/T^2$ is chosen rather than ν^*.

In this exercise, in addition to q_{cyl}, β, Mach number ($M_\phi=R.\omega_{tor}/c_s$) are maintained constant throughout as well as the plasma cross-section and aspect ratio. Thus, the total energy content $W=3.\beta_N.B_T.V.I_p/(200.a.4\pi\mu_o)$ is inferred directly from the imposed normalised pressure. The density normalised to the Greenwald density ($\pi a^2n/I_p$) is not considered as a constraint. It must be pointed out that the last hypothesis (conservation of the Mach number) are likely to be too optimistic as it is expected to be lower in ITER and known to be favourable in reducing the core transport.

The fusion power calculation uses the CRONOS suite of codes [5]. In these computations, the scaled temperature and density profiles are given as input at each step, to keep the dimensionless parameters constant. The plasma equilibrium is calculated for each step (identity, ρ* and ν*), and the fusion power calculated using the Bosch-Hale formulation within CRONOS. The standard assumption regarding radiation and Zeff for ITER are used: the discharge contains Be (2%) and Ar (0.12%) impurities, tied to the electron density profiles; the He profile is calculated by a 1D diffusion equation which imposes a ratio of 5 between the He particle confinement time and the global energy confinement time. This leads to a total effective mass of 1.65. The Zeff measured in 77933 is 2.07. The plasma is comprised of a 50:50 D:T ratio.

	77933 (2.3T)	**CRONOS**	**Identity**	**ρ* step**	**ν* step**
a (m)	0.93	0.93	1.981	1.982	1.982
R (m)	2.905	2.905	6.199	6.199	6.199
I (MA)	2	2	1.655	6.029	9.954
B (T)	2.27	2.27	0.881	3.21	5.3
Vol (m^3)	75.78	75.75	733.835	733.83	731.135
a/R	0.320	0.320	0.320	0.320	0.320
κ	1.53	1.53	1.551	1.550	1.547
I/aB	0.947	0.947	0.948	0.948	0.948
n ($10^{\wedge 20} m^{-3}$)	0.544	0.544	0.120	0.670	0.685
Greenwald fraction	0.739	0.739	0.892	1.372	0.849
q_{cyl}	2.582	2.582	2.614	2.615	2.610
ρ*	4.8810^{-3}	5.0410^{-3}	5.0710^{-3}	2.3810^{-3}	2.3710^{-3}
β	2.1610^{-2}	2.2810^{-2}	2.3310^{-2}	2.3210^{-2}	2.3210^{-2}
ν_c	7.8210^{-1}	7.0210^{-1}	6.7610^{-1}	6.8610^{-1}	9.7010^{-2}
ω_c [rd/s]	$1.16\ 10^5$	1.16105	-	-	-
W_{th} [MJ]	5.034	5.312	7.898	103.880	284.350
P_{FUS} [MW]	-	-	0.038	34	477.83
Q				**0.68**	**9.54**

Under the present analysis it looks feasible to reach significant gain factor Q=9.54 with a scenario at moderate current. This prediction is consistent with other extrapolations made in ASDEX Upgrade [22] and DIII-D [23]. The hypotheses used have been examined by sensitivity studies on Zeff, Ti/Te and estimated for the rotation. Choosing Zeff=2.07 (as in 77933) instead of 1.65 (by increasing the Be and Ar concentrations) leads to a reduction of the fusion power by 20% primarily by fuel dilution. Setting Te=1.1Ti while keeping the energy content constant has the effect to decrease the fusion power by typically 20%. The largest uncertainty remains the rotation for which there could be a reduction of the fusion power by 30% according to GLF23 calculations made with zero rotation in ITER. In total, with the above uncertainties, the fusion power can exceed 50%. Density peaking is another additional source of uncertainty at low collisionality which may affect also the final results [24]. To reduce these uncertainties, the extrapolations should therefore start from discharges having similar Ti/Te and Mach number than that expected in ITER and explore the ρ* and ν* scaling across the existing machines.

6. Summary and significance for ITER.

The recent JET hybrid scenario experiments have achieved confinement performance giving more confidence in the feasibility of this scenario for both low and high triangularity. However, these two cases are operated in a different parameter space and the origin of the good performance is different. For the low shape case, the core transport seems to play an important role thanks to their high rotation and Ti/Te. In addition the pedestal confinement has a stronger dependence with the input power. The high triangularity may also benefit from the core transport, but less than the low shape case due to its lower rotation gradient and Ti/Te. In the high triangularity case, the minimisation of the plasma-wall interaction has had also a large impact on the pedestal performance in the most recent experiments. In both cases the q profile broadening has been instrumental in developing stable discharges with regard to the NTMs. Although JET has not yet operated in the ITER domain in terms of Ti/Te and rotation, the results are suggesting that there is good prospect to produce in ITER long pulse operation at reduced current which may be extrapolated to an acceptable fusion gain despite having a large error bar.

This implies important conditions: 1- it appears clearly that the control of the off-axis current (using ECCD for example) is essential in ITER at around r/a~0.5 to ensure the stability of the scenario and possibly optimise the transport in the core [25]. 2- The rotation and momentum transport predictions [26] of ITER remain an essential element for the confinement predictions. This is at present the main uncertainty in the extrapolations. 3- The present data on the hybrid scenario have been collected in a carbon wall which has been shown to influence the pedestal confinement. The results presented here need to be repeated and consolidated in a metallic wall in beryllium and tungsten where the edge conditions are likely to be radically different. 4- The physics parameter dependence of the present H98y2 scaling does not describe well the new hybrid results. This makes the 0D extrapolation very uncertain at high normalised pressure in particular. It is therefore important to develop further the dedicated dimensionless scaling [21] with the hybrid scenario in particular with ν^* across the present machines and having Ti/Te ratio and rotation that are compatible with what will be produced in ITER.

7. Reference

[1]: ITER Physics basis, Nucl. Fusion **39** No 12 (December 1999) 2175-2249
[2]: E. Joffrin et al 2005 Nucl. Fusion **45** 626
[3]: D. McDonald et al., 2008 Plasma Phys. Control. Fusion 50 124013
[4]: P. Politzer, this conference, EXC/P2-06
[5]: J.F. Artaud et al, 2010, Nuc. Fusion 50 043001
[6]: R. V. Budny et al 1992 Nucl. Fusion **32** 429.
[7]: T. C. Luce et al., Nuc. Fusion **43** (2003) 321
[8] : Y. Su-Na, Nuc Fusion 46 (2006) 232
[9] : G. Garcia et al., Phys. Rev. Lett. 104 (2010) 205003
[10]: SC Guo, et al., Phys. Fluids B **5** (1993) 520
[11]: M. Kotschenreuther et al., Comput. Phys. Commun. 88 (1995) 128
[12]: P. Mantica, Phys. Rev. Lett. **102**, 175002 (2009) and this conference EXC/9-2
[13]: J.E Kinsey, Physics of Plasma 13 022305 (2006)
[14]: J. Stober et al., Nuc. Fusion **47** (2007) 728
[15]: H. Lütjens., J.-F. Luciani and X. Garbet Phys.Plasmas 8 4267–70 (2001) and P. Maget et al., this conference EXS/P5-09
[16]: L. Frassinetti et al., 37th EPS Conference on Plasma Phys. Dublin, 2010, P-1.1031
[17]: D. McDonald et al, Plasma Phys. Control. Fusion 46 (2004) A215 and McDonald D. 12th International Workshop on "H-mode Physics and Transport Barriers", Princeton 2009.
[18]: R. Simonini, G. Corrigan, G. Radford, J. Spence and A. Taroni. *Cont. to Plasma Phys.* **34** (1994), p. 368
[19]: A. Huber et al., Journal of Nuclear Materials, Volumes 290-293, March 2001, Pages 276-280,
[20]: C. Challis, APS 2009 November 2 - 6, 2009 Atlanta, Georgia
[21]: T. C. Luce PPCF, 50 (2008) 043001
[22]: G. Tardini, 2009 *Nucl. Fusion* **49** 075004 and ACC Sips et l., 2007 *Nucl. Fusion* **47** 1485
[23]: E. Doyle et al, 2010 *Nucl. Fusion* **50** 075005
[24]: M. Maslov et al. Nuc Fus 49 (2009) 075037
[25]: T. Tala et al, this conference
[26]: J. Citrin et al, accepted for publication in Nuc Fus 50 (2010).

---

* See the Appendix of F. Romanelli et al., Proceedings of the 22nd IAEA Fusion Energy Conference 2008, Geneva, Switzerland.